International Journal of Heat and Mass Transfer 73 (2014) 542–550

Contents lists available at ScienceDirect

International Journal of Heat and Mass Transfer

journal homepage: www.elsevier.com/locate/ijhmt

Effects of flow field on the wall mass transfer rate behind a circular orifice in a round pipe

Feng Shan *, Atsushi Fujishiro, Tatsuya Tsuneyoshi, Yoshiyuki Tsuji

Department of Energy Engineering and Science, Nagoya University, Nagoya 464-8603, Japan

ARTICLE INFO

Article history:
Received 27 August 2013
Received in revised form 15 February 2014
Accepted 16 February 2014
Available online 14 March 2014

Keywords:
Wall mass transfer
Orifice flow
Flow-accelerated corrosion
Separated flow

ABSTRACT

We simultaneously measured the flow field and wall mass transfer rate behind an orifice by means of particle image velocimetry (PIV) and the limiting diffusion current technique (LDCT), respectively. The spatio-temporal correlation coefficients of the local vertical velocity and the wall mass transfer are presented, and the canonical correlations between the proper orthogonal decomposition (POD) spatial eigenmodes in the recirculation region and the wall mass transfer rate are also discussed. A response time lag occurs between the wall mass transfer rate and the velocity field. The large canonical correlation between the POD eigenmodes and wall mass transfer rate suggests that large-scale flow structures are important to the wall mass transfer rate. In addition, the second eigenmode in the recirculation region is responsible for the peak of the mean wall mass transfer rate.

1. Introduction

Mass transfer between a solid boundary and the turbulent fluid flowing over it, hereafter denoted as the wall mass transfer rate, is a fundamental problem in fluid mechanics and chemical engineering. However, it is very challenging to build a theory that relates the wall mass transfer rate to the velocity field, as reported by Campbell and Hanratty [1]. Hanratty [2] determined that the wall can be considered as an array of point sources and sinks when discussing the heat or mass transfer between a wall and a turbulently flowing fluid. This finding promoted an attempt to study the behaviors of small wall sources [3,4]. A widely used approach to measure the wall mass transfer rate is the introduction of a chemical solution by conducting an electrochemical reaction on a small circular electrode embedded in the wall so that the flow is not disturbed. If the composition of the chemical solution is carefully controlled, the polarographic method, which was awarded the Nobel Prize for chemistry in 1959, can be used to quantitatively measure the transport property at the wall.

In separated internal flows, such as flows in sudden pipe expansions and those behind orifices, the mean value of wall mass transfer rate is usually greatly enhanced and reaches the maximum value at some distance downstream of the separation point before decreasing to the fully developed value. Several researches focused on the empirical regression of the enhanced mass/heat transfer process as a function of nondimensional parameters, i.e., describing the Sherwood number (Nusselt number) as a function of Reynolds number and Schmidt number (Prandtl number) [5–10]. Recently, Ahmed et al. [11] reported that the downstream variations of pipe-wall thinning behind an orifice are strongly correlated with the turbulence energy, and Utanohara et al. [12] determined that such thinning is correlated with the fluctuating wall shear stress in the flow. Pipe-wall thinning due to flow-accelerated corrosion (FAC) is currently considered as a mass transfer phenomenon in which the ferrous ions from the wall materials of carbon steel are included in the bulk flow [11,12]. The mass transfer coefficient of the flow behind an orifice was measured by using the naphthalene sublimation method [13,14], which allows for measurement of the mass transfer coefficient in the air flow at a low Schmidt number ($Sc = 2.3$). Yamagata et al. [15] conducted both experimental and numerical studies on the mass transfer characteristics behind an orifice in a circular pipe for application to pipe-wall thinning. More specifically, they measured the mass transfer coefficient behind the orifice by using the benzoic acid dissolution method, which allows for measurement of the mass transfer coefficient at a Schmidt number of approximately 300. Moreover, they analyzed the effects of the Schmidt and Reynolds numbers on the mass transfer characteristics by using a combination of the k–ε turbulence model and the empirical model of high Schmidt number flow.

Few studies focus on the reasons for the occurrence of a peak mean wall mass transfer rate in separated internal flows. Ma et al. [16] determined that heat transfer in the recirculation region

* Corresponding author. Tel.: +81 52 789 4679.
E-mail address: shan.feng@e.mbox.nagoya-u.ac.jp (F. Shan).

http://dx.doi.org/10.1016/j.ijheatmasstransfer.2014.02.039

was maximum near the area in which wall shear was minimal. Although no conclusive reasons have been reported for the obvious peak in the wall mass transfer rate in separated flows, the existence of the peak mean wall mass transfer rate is believed to be associated with many important transport properties in separated internal flows. For example, data published by many researchers strongly suggest a close relationship between the wall mass transfer rate and observed FAC rates [8,10]. Therefore, a nonuniform profile of the mean wall mass transfer rate downstream of the separation could result in nonuniform pipe-wall thickness and thus pipe rupture at the location of thinnest pipe wall, particularly in chemical and energy applications [17,18].

The present study is part of continuous research based on separate measurements of flow field by particle image velocimetry (PIV) [19,20] and wall mass transfer rate by the limiting diffusion current technique (LDCT) [21] on two flow loops with the exact same hydrodynamic conditions. In the present study, we first explore the reason for the peak mean wall mass transfer rate position downstream of an orifice from the perspective of flow field. In addition, we explore the response of the wall mass transfer rate to the velocity field by simultaneously measuring the flow field and wall mass transfer rate.

To the best of our knowledge, precise data on the flow field and wall mass transfer rate simultaneously measured behind an orifice have not been reported thus far. We believe that this study provides a basic and important experimental database for understanding the FAC problem within the recirculation region bounded by an axisymmetric shear layer. In addition, this study serves as a useful reference for building a theory to relate the flow field and wall mass transfer rate in separated internal flows. Although we examine only mass transfer in this study, it is possible to extend the main results to heat transfer due to analogies among the transport phenomena.

2. Experimental setup

2.1. Test section for simultaneous measurement of flow field and wall mass transfer rates

The hydrodynamic conditions of the flow recirculation loop in the present study are the exact same as those previously used [19,20]; however, the test section was custom designed. Fig. 1 shows the test section as well as the experimental coordinate system. As shown in the figure, the Cartesian coordinate system was used with the origin located at the center of the downstream surface of the orifice plate. x, y, and z represent the streamwise, vertical, and spanwise directions, respectively, and u, v, and w represent the streamwise, vertical, and spanwise components of instantaneous velocity, respectively. The test section housed the electrodes, among which one working cathode was located at $3D$ from the upstream surface of the orifice plate, where D is the pipe's inner diameter, and several working cathodes were located downstream of the orifice plate. From $0.1D$ to $2D$ downstream of the orifice plate, the distance between neighboring cathodes was $0.1D$, whereas that in the region from $2D$ and $3D$ was $0.2D$. All working cathodes were constructed by inserting a cylindrical gold wire with a diameter of 1 mm into the pipe wall. The counter and reference electrodes were located approximately five and eight times the pipe diameter away from the downstream surface of the orifice, respectively. The counter electrode (anode) was a nickel circular ring with a thickness of 5 mm. The relatively large size of the counter electrode (anode), compared with that of the cathodes, was selected to ensure that the current flowing into the circuit was controlled by reactions at the cathode surface. All electrodes were mounted flush with the pipe wall; therefore, no abrupt change of the hydrodynamic conditions occurred in the connection region between the electrodes and the pipe wall. The visualization area of the PIV measurement as shown by ⑤ in Fig. 1 was $4.4R \times 2R$, where $R \equiv D/2$ is the pipe radius.

Fig. 2 shows a sketch of the stereo-PIV system from the top view, in which only the first and the last downstream electrodes are shown for a clearer presentation of the laser sheet. In addition to the water tank surrounding the pipe, two water-filled prisms were set to further reduce the optical distortion in the stereo-PIV measurements. Similar water-filled prisms were used for stereo-PIV measurements in previous studies [22]. The reasons for prism usage to reduce optical distortion have been previously reported [23]. We used the experimental setup shown in Fig. 2 to conduct measurements of statistical quantities of the flow field, and simultaneous measurements of the flow field and wall mass transfer. It is nearly impossible to validate the accuracy of an instantaneous velocity field measured by stereo-PIV in turbulence. Therefore, we calculated the statistical quantities of the flow field measured by stereo-PIV and compared the results with those obtained by planar PIV to validate the accuracy. Very good agreements have been previously reported [20]. Because the parameters of the hardware used in the statistical measurements have also been previously reported [19], in this paper we present only the parameters of the hardware used in the simultaneous measurements.

2.2. Experimental conditions for PIV and LDCT

We first used a commercial potentiostat (PGSTAT12, Metrohm Autolab Co.) to measure the current–voltage relationship at each local working cathode to obtain the range of voltage in which the current is mass-transfer controlled and the profile of the mean wall mass transfer rate. We then determined the location of the maximum mean wall mass transfer rate and denoted this location as x_{max}. We next conducted simultaneous measurements of velocity field and single-point wall mass transfer rate at x_{max}. A handcrafted potentiostat was employed to maintain constant voltage between the anode and the local cathode, and the value of the voltage

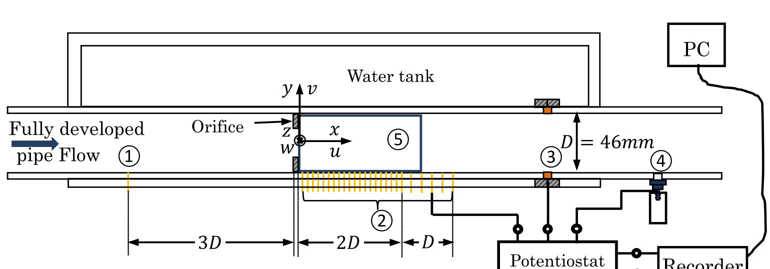

Fig. 1. Sketch of the test section (front view): ① upstream electrode (cathode); ② downstream electrodes (cathode); ③ counter electrode (anode); ④ reference electrode; ⑤ PIV measurement area ($4.4R \times 2R$).